

Alpha and alpha-beta phase synchronization mediate the recruitment of the visuospatial attention network through the Superior Longitudinal Fasciculus

Antea D'Andrea ^{a,b}, Federico Chella ^{a,b}, Tom R. Marshall ^c, Vittorio Pizzella ^{a,b}, Gian Luca Romani ^b, Ole Jensen ^d, Laura Marzetti ^{a,b,*}

^a Department of Neuroscience, Imaging and Clinical Sciences, "G. D'Annunzio University" of Chieti-Pescara, 66100, Chieti, Italy

^b Institute for Advanced Biomedical Technologies, "G. D'Annunzio University" of Chieti-Pescara, 66100, Chieti, Italy

^c Department of Experimental Psychology, University of Oxford, Oxford, OX1 3PH, United Kingdom

^d School of Psychology, University of Birmingham, Hills Building, Birmingham, B15 2TT, United Kingdom



A B S T R A C T

It is well known that attentional selection of relevant information relies on local synchronization of alpha band neuronal oscillations in visual cortices for inhibition of distracting inputs. Additionally, evidence for long-range coupling of neuronal oscillations between visual cortices and regions engaged in the anticipation of upcoming stimuli has been more recently provided. Nevertheless, on the one hand the relation between long-range functional coupling and anatomical connections is still to be assessed, and, on the other hand, the specific role of the alpha and beta frequency bands in the different processes underlying visuo-spatial attention still needs further clarification.

We address these questions using measures of linear (frequency-specific) and nonlinear (cross-frequency) phase-synchronization in a cohort of 28 healthy subjects using magnetoencephalography. We show that alpha band phase-synchronization is modulated by the orienting of attention according to a parieto-occipital top-down mechanism reflecting behavior, and its hemispheric asymmetry is predicted by volume's asymmetry of specific tracts of the Superior-Longitudinal-Fasciculus. We also show that a network comprising parietal regions and the right putative Frontal-Eye-Field, but not the left, is recruited in the deployment of spatial attention through an alpha-beta cross-frequency coupling. Overall, we demonstrate that the visuospatial attention network features subsystems indexed by characteristic spectral fingerprints, playing different functional roles in the anticipation of upcoming stimuli and with diverse relation to fiber tracts.

1. Introduction

The selection of relevant information, while inhibiting distracting input, is necessary to act in everyday life. The coordinated activity of different brain areas in brain networks seems necessary to instantiate the cognitive functions involved in this process (Corbetta and Shulman, 2002). It has been hypothesized that this coordinated activity is maintained through synchronization of neuronal oscillations in several cognitive domains (Varela et al., 2001; Fries, 2005; Engel et al., 2013), including attentional selection (Engel et al., 2001; Salinas and Sejnowski, 2001; Fries, 2015), and can thus be observed with magnetoencephalography (MEG) or electroencephalography (EEG). Specifically, local neuronal oscillations at low frequencies, especially in the alpha band (8–12 Hz), have been observed over the visual cortex in anticipation of distracting input (Worden et al., 2000; Wyart and Tallon-Baudry, 2008) and have been related to functional inhibition (Jensen and Mazaheri, 2010). Along the same line, attentional modulation in the anticipation of upcoming stimuli of MEG alpha band oscillation has also been reported over the parietal cortex. These local alpha band activity

modulations in visual and parietal cortices are behaviorally relevant, e.g., an improvement in target detection has been observed in the hemifield to which attention is directed (Thut et al., 2006; Sauseng et al., 2005).

Yet, orienting attention to a spatial location is a process that is known to recruit not only primary cortices, but also other areas within a frontoparietal circuit (Bushnell et al., 1981; Corbetta and Shulman, 2002; Kastner and Ungerleider, 2000). While evidence for local alpha band synchronization is abundant (Jensen et al., 2015), less studies have investigated inter-areal synchronization during the anticipation of upcoming stimuli with MEG or EEG (Doesburg et al., 2009; Siegel et al., 2008; Sacchet et al., 2015; Lobier et al., 2018). In these studies, different frequencies in the alpha to beta range have been proposed as the carrier frequency for the functional integration mechanism. A recent MEG study from Lobier et al. (2018) reported inter-areal phase synchronization between frontal, parietal and visual regions in the high alpha (10–14 Hz) but not in the low alpha (6–9 Hz) frequency band in a group of 14 subjects. The seminal work from Siegel et al. (2008) reported MEG modulations of alpha (5–15 Hz) and beta (15–35 Hz) band phase

* Corresponding author. Institute for Advanced Biomedical Technologies, "G. d'Annunzio University" of Chieti-Pescara, via Luigi Polacchi 11, 66100, Chieti, Italy.
E-mail address: laura.marzetti@unich.it (L. Marzetti).

coherence between middle-temporal and parietal areas in stimulus anticipation in 8 subjects. The observed modulations were larger ipsilaterally to the attended side consistently with an inhibitory role. Moreover, Sacchet et al. (2015) found that alpha (7–14 Hz) and beta (15–29 Hz) synchronization between primary somatosensory areas and right prefrontal cortex in a group of 12 subjects are enhanced to serve functional inhibition. In monkey studies, evidence has been provided for a top-down inter-areal synchronization between frontal and parietal areas in the beta band at different frequencies: 22–30 Hz in Buschman and Miller (2007) and 14–18 Hz in Bastos et al. (2015). In this framework, it is clear that the debate regarding the specificity of these frequencies, regions and direction of modulations in long-range synchronization is still open, and the specific role of the two bands is not yet clear (Fries, 2015).

Additionally, no evidence exists for the relationship between long-range functional synchronizations and its putative anatomical substrate. In fact, while the Superior Longitudinal Fasciculus (SLF) has been proposed as the structural connection between prefrontal regions and posterior areas (Thiebaut de Schotten et al., 2011), and its relation to synchronization of neuronal population at a local scale, as indexed by signal power, has been reported (Marshall et al., 2015), the role of SLF tracts in long-range inter-areal synchronization is still to be demonstrated.

In the present study, we aim at reconciling the previous findings on the different frequencies and regions involved in inter-areal phase synchronization by investigating frequency specific and cross-frequency phase-synchronization, and by exploring their relation to the SLF anatomical substrate in 28 healthy participants.

Specifically, using magnetoencephalographic data and a multivariate measure of linear coupling (Ewald et al., 2012; Marzetti et al., 2013), we quantify functional connectivity between neuronal oscillations of brain activity in the alpha and beta frequency bands. Additionally, by using a measure of nonlinear phase-coupling, i.e., antisymmetric cross-bicoherence (ACB; Chella et al., 2014; Chella et al., 2016), we assess cross-frequency interactions between alpha and beta bands to account for higher order functional mechanisms. Finally, the relationship of frequency-specific functional connectivity to individual differences in anatomical characteristics of SLF and to performance is assessed.

Overall, our study reveals, a cross-frequency coupled alpha-beta fronto-parietal system for the deployment of visuospatial attention, and an alpha band parieto-occipital system related to the orienting of attention. The latter is mediated by SLF anatomical tracts and is behaviorally relevant. Thus, the visuospatial attention network features functional subsystems indexed by characteristic spectral fingerprints which play different roles in the anticipation of upcoming stimuli and rely on specific anatomical substrates.

2. Methods

2.1. Participants

Twenty-eight right-handed subjects (15 males, 13 females, age: mean value 24 y and 5 mo, standard deviation 3 y and 5 mo) participated in the experiment. All subjects were naïve for the performed task. All subjects underwent the standard screening procedures for MEG and MRI (structural and diffusion). The local Ethics Board approved all recruitment and assessment procedures (CMO region Arnhem-Nijmegen, CMO2001/095). All subjects, after receiving a comprehensive description of the study and asking questions, provided written informed consent. Experiments were carried out in accordance with the Declaration of Helsinki. Two of the enrolled subjects were excluded from the analysis of diffusion MRI, one because he/she did not complete the diffusion scanning and one because the SLF branches could not be reconstructed. Therefore, the multimodal analyses were conducted only on 26 subjects out of the full 28 subjects' cohort. The same data have been used in (Marshall et al., 2015).

2.2. Stimulus material and procedure

Behavioral cueing task. Subjects performed a cued visuospatial attention task (Fig. 1). At all times, two luminance pedestals were present on the screen at 3.2° of visual angle below the horizontal meridian and 4.8° of visual angle to the left and right of the vertical meridian. Each trial began with the presentation of visual cues (one target patch and one distractor patch) presented to the left and right side of a central fixation dot. These cues instructed the subject to either attend to the left pedestal ("Attend Left" cue) or to the right pedestal ("Attend Right" cue). A pair of target Gabor patches with a spatial frequency of four cycles per degree visual angle were presented at each luminance pedestal for 60 ms, followed by a 60 ms mask, after a 1500 ms delay interval. The target patch was tilted 45° either clockwise or anticlockwise. The distractor patch was either horizontal or vertical. All target patches were presented at the cued luminance pedestal (i.e., 100% valid cues). Subjects had to report the orientation of the target patch by a right-hand button press (index finger for clockwise orientation, middle finger for anticlockwise orientation). In total, the task consisted in 13 blocks of 40 trials (with short breaks between different blocks) and lasted approximately 50 min.

2.3. MEG

MEG data acquisition. MEG data were acquired using a whole-head MEG system with 274 axial gradiometers (CTF275-channel MEG system, VSM MedTech) at a sampling rate of 1200 Hz. Ear canal and nasion markers were used to continuously monitor head position during acquisition with a real-time head localizer tool (Stolk et al., 2013). An

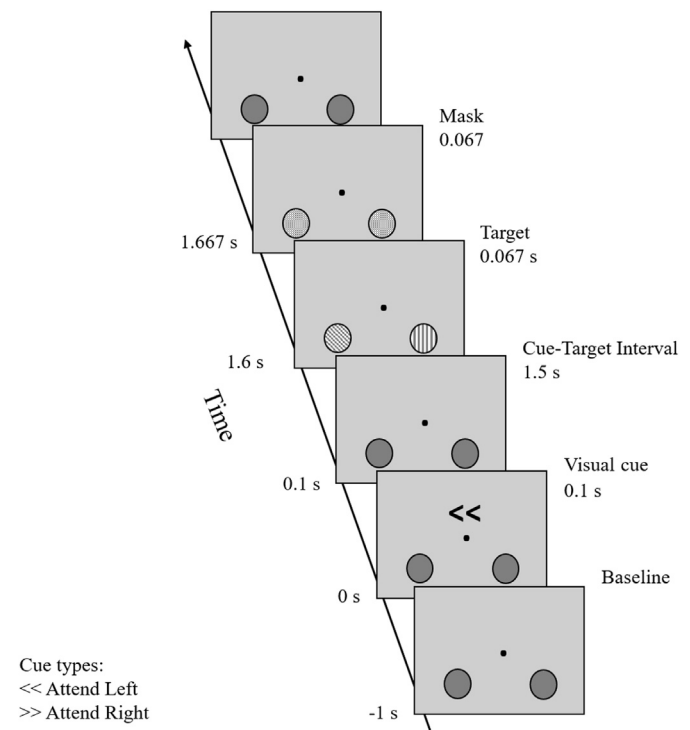


Fig. 1. Experimental paradigm. Each of the trials considered for this study began with a visual cue, instructing the subject to attend either to the left luminance pedestal or to the right luminance pedestal. After a 1.5 s fixed time interval, a pair of Gabor patches appeared in both luminance pedestals. One of them (target) was always 45° oriented (clockwise or counterclockwise from vertical), and the other cardinally oriented (horizontal or vertical). In the "Attend Left" and "Attend Right" conditions, the diagonal patch appeared respectively in the left or right pedestal, thus always leading to 100% cue validity. Subjects had to discriminate the orientation of the diagonal patch. See also Marshall et al. (2015).

EyeLink 1000 eyetracker (SR Research, Ottawa, Canada) was used to continuously track the left eye for eye blink and saccade detection. Additional specific information about the MEG data acquisition can be found in Marshall et al. (2015).

MEG data analysis. MEG data were first preprocessed to exclude trials containing flux jumps of the detector, muscular activity, eye blinks and horizontal movements (Marshall et al., 2015). In the present study, we additionally run an Independent Component Analysis (ICA) based on logistic infomax algorithm (runica, Bell and Sejnowski, 1995; Makeig et al., 1996), in order to remove other biological and instrumental artifacts. Particular attention was paid to the removal of heart related activity due to its possible influence on connectivity results (Gross et al., 2013). The Fieldtrip Matlab toolbox (Oostenveld et al., 2011) was used for MEG data artifact removal. This procedure led to an average across subjects of 100 artifact free trials for the “Attend Left” condition and of 101 artifact free trials for the “Attend Right” condition to be used for the following analyses.

MEG source-level analysis was performed by using frequency domain DICS beamforming (Gross et al., 2001) and sources located at the vertices of a regular 6 mm grid uniformly distributed in the MNI space. To allow direct averaging across subjects, the single subject grids were derived from a common template grid constructed using a MNI template brain (Fonov et al., 2009, 2011). Specifically, for each subject, the source grid was produced by warping the individual anatomical MRI scans to this template and applying the inverse warp transformation to the template grid. This resulted in source grids aligned across subjects in the MNI space. The MEG forward problem was solved by using the leadfield method based on a single shell head model (Nolte, 2003). To construct a spatial filter which projects data from the sensor-level to the source-level, we considered segments of data of 1 s from the pre-cue interval (−1.00, 0.00 s) and the cue-target interval (0.45, 1.45 s), given previous evidence for alpha power modulation in the same data segments (Marshall et al., 2015). Cross-spectral density matrices in the alpha band were computed from sensor signals using a set of three orthogonal Slepian tapers with a 10 Hz center frequency to produce 2 Hz frequency smoothing (i.e., 8–12 Hz alpha band) (Percival and Walden, 1993). A common spatial filter was constructed using cross-spectral density estimated from pre-cue interval and the cue-target intervals and all conditions, with the Fieldtrip Matlab toolbox (Oostenveld et al., 2011). Finally, source-level cross-spectral densities were estimated for each time window and for each trial conditions by projecting the respective sensor-level cross-spectral densities through the common spatial filter.

MEG alpha band connectivity analysis. As a general remark, it should be noted that if no a priori assumption is made on the orientation of brain sources, MEG brain signals at each source location and for each time point are multidimensional, i.e., they represent the activity of source components in three orthogonal directions, as opposite to e.g. signals from functional Magnetic Resonance which are scalar values. In order to estimate functional connectivity between two sources, multivariate measures which take into account the coupling between three-dimensional quantities are thus better suited than applying dimensionality reduction approaches and bivariate functional connectivity methods (Marzetti et al., 2013).

Specifically, for functional connectivity based on spectral properties the cross-spectral density between three-dimensional source signals at one brain location consists in a 3×3 matrix collecting the cross-spectra between all the possible combinations of the three orientations from this location. Indeed, in this study, functional connectivity in the alpha band was derived from these source-level cross-spectral densities by the Multivariate Interaction Measure (MIM) (Ewald et al., 2012; Marzetti et al., 2013). MIM is based on the maximization of the imaginary part of coherence (Nolte et al., 2004) between the two multidimensional signals, and is thus a quantity robust to mixing artifacts. When interested in functional connectivity between brain sources, mixing artifacts correspond to source leakage (Colclough et al., 2015), i.e. the spread over several voxels of the reconstruction of a point like dipole source, which

induces artificial connectivity patterns (Schoeffelen and Gross, 2009; Palva and Palva, 2012). Source leakage is indeed instantaneously coupled to source activities, it is thus straightforward to notice that a non-vanishing imaginary part of coherence cannot be explained only by source leakage since these systematically ignores functional relations occurring at zero-phase delays, including zero-phase genuine interactions.

Here, to investigate functional coupling with the visual cortex, we selected as reference region the posterior region identified as the Superior Occipital Cortex (SOC) in (Marshall et al., 2015), i.e. according to the parcellation of the Automated Anatomical Labeling (AAL) atlas (Tzourio-Mazoyer et al., 2002). MEG functional connectivity between this region and all the other voxels in the brain was estimated using the MIM (Marzetti et al., 2013; Andreou et al., 2015; Peiker et al., 2015; Brunetti et al., 2017) in the alpha band, according to Eq. (1):

$$\text{MIM}_{ij}(f) = \text{trace} \left(\left(C_{ii}^R(f) \right)^{-1} C_{ij}^I(f) \left(C_{jj}^R(f) \right)^{-1} \left(C_{ij}^I(f) \right)^T \right) \quad (1)$$

where C_{ii} and C_{jj} are the 3×3 cross-spectra between the signal at location i or j and itself, and C_{ij} is the cross-spectrum between the signal at location i and at location j . In the above notation, *trace* indicates matrix trace, superscripts R and I denote the real and the imaginary parts, and superscripts T and -1 indicate matrix transpose and inverse, respectively. The MIM between the SOC and a given target brain voxel j , namely $\text{MIM}_{\text{SOC},j}$, was calculated as the average of the MIM values obtained for the N voxels that fall within the SOC parcel, i.e., $N = 48$ for the left and $N = 58$ for the right hemisphere SOC, for a $6 \times 6 \times 6 \text{ mm}^3$ source space resolution, and the target voxel j for the “Attend Left” trials and for the “Attend Right” trials, separately.

To investigate the modulations of connectivity induced by the cue presentation, we performed a contrast, hereinafter referred to as modulated MIM (mMIM), between the MIM connectivity values in the cue-target interval (450–1450 ms post-cue presentation, thus avoiding the possible contamination from evoked activity) and the respective values in the baseline (defined as a 1 s window prior to cue presentation). Given that our interest is to investigate connectivity modulations related to ipsilateral inhibition, we calculated whole brain mMIM values with respect to the left hemisphere SOC (lSOC) for the “Attend Left” condition and with respect to right hemisphere SOC (rSOC) for the “Attend Right” condition, according to:

$$\text{mMIM}_{\text{lSOC},j}^{\text{AttendLeft}} = \text{MIM}_{\text{lSOC},j}^{\text{AttendLeft}} - \text{MIM}_{\text{lSOC},j}^{\text{Baseline AttendLeft}} \quad (2)$$

$$\text{mMIM}_{\text{rSOC},j}^{\text{AttendRight}} = \text{MIM}_{\text{rSOC},j}^{\text{AttendRight}} - \text{MIM}_{\text{rSOC},j}^{\text{Baseline AttendRight}} \quad (3)$$

The statistical significance of the observed differences was assessed by cluster-based permutation statistic (see Experimental Design and Statistical Analysis section). For an efficient implementation of the MIM estimation, the cross-bispectral densities and the signal Fourier coefficients were first estimated at the sensor-level and then projected at the source-level through the frequency domain DICS beamforming spatial filter derived as described above in the **MEG data analysis** section. To evaluate whether modulation of MIM can be biased by power modulations, we run a control analysis in which the statistical significance of mMIM results was assessed after linear regression of power modulations.

Additionally, we used the Phase Slope Index (PSI; Nolte et al., 2008), a measure of directional connectivity the sign of which informs about which signal is temporally leading which, to assess the dominant direction of the observed interaction. Specifically, given two brain voxels, we considered the signal projections along orthogonal directions in each voxel set according to maximal imaginary coherence between the two voxels (Ewald et al., 2012). We then calculated the PSI for all pairwise combinations of the two signal projections from these two voxels, and then averaged all pairwise combinations (Basti et al., 2018). The PSI

between the SOC parcel and a given target voxel j , i.e., $\text{PSI}_{\text{SOC},j}$, was then evaluated as the mean of the PSI values between j and all the voxels falling within the SOC parcel.

To assess the frequency specificity of the connectivity modulations, we calculated the Time Frequency Representation (TFR) of the mMIM values in eq. (2) and eq. (3). TFRs were calculated by the Fieldtrip software toolbox (Oostenveld et al., 2011), using a sliding window approach with a time window of variable length for different frequencies. Here, all time windows were designed to contain five cycles of the corresponding oscillation for each frequency in the range [0 80] Hz. Hanning tapering was used for all windows. Given that for this analysis the whole band data are required, to derive source space timecourses a broadband spatial filter was constructed by using a time-domain Linearly Constrained Minimum Variance (LCMV) beamforming (Van Veen et al., 1997). The covariance matrix and the regularization for the LCMV are the same used for the cross-frequency analysis described in the next paragraph.

Finally, in order to quantify whether the observed modulation of functional connectivity is specific to the attended side, we computed an attentional modulation index for the mMIM, namely the functional connectivity Attentional Modulation Index (fcAMI), defined as:

$$\text{fcAMI}_{\text{ISOC},\text{IX}}^{\text{AttendRight} - \text{AttendLeft}} = \frac{1}{N_{\text{IX}}} \sum_{j \in \text{IX}} \frac{\text{mMIM}_{\text{ISOC},j}^{\text{AttendRight}} - \text{mMIM}_{\text{ISOC},j}^{\text{AttendLeft}}}{|\text{mMIM}_{\text{ISOC},j}^{\text{AttendRight}}| + |\text{mMIM}_{\text{ISOC},j}^{\text{AttendLeft}}|} \quad (4)$$

$$\text{fcAMI}_{\text{rSOC},\text{IX}}^{\text{AttendLeft} - \text{AttendRight}} = \frac{1}{N_{\text{RX}}} \sum_{j \in \text{RX}} \frac{\text{mMIM}_{\text{rSOC},j}^{\text{AttendLeft}} - \text{mMIM}_{\text{rSOC},j}^{\text{AttendRight}}}{|\text{mMIM}_{\text{rSOC},j}^{\text{AttendLeft}}| + |\text{mMIM}_{\text{rSOC},j}^{\text{AttendRight}}|} \quad (5)$$

where the index j runs over all the voxels in the AAL parcel corresponding to the regions found to be modulated by the cue presentation in the mMIM analysis and indicated by X in the above Eq. (4) and Eq. (5).

Additionally, cue-induced modulation of functional connectivity in the beta band (13–30 Hz) with respect to the SOCs was assessed with the same approach.

MEG cross-frequency analysis. To investigate cross-frequency coupling, we relied on the magnitude of the antisymmetric cross-bicoherence (ACB) between source signals (Chella et al., 2016). The ACB is a measure of the cross-frequency synchronization (Nikias and Petropulu, 1993) between signal components at two frequencies f_1 and f_2 and at their harmonically coupled frequency $f_3 = f_1 + f_2$, and represents the extension of the imaginary part of coherence to the cross-frequency case, resulting thus robust to mixing artifacts (Chella et al., 2014; Soto et al., 2016). ACB in this work is calculated as in the following Eq. (6):

$$\begin{aligned} \text{ACB}_{i,j}(f_1, f_2) &= \left| \frac{B_{i,j}(f_1, f_2) - B_{j,i}(f_1, f_2)}{\mathcal{N}_{i,j}(f_1, f_2)} \right| \\ &= \left| \frac{\langle s_i(f_1) s_i(f_2) s_j^*(f_1 + f_2) \rangle - \langle s_j(f_1) s_i(f_2) s_i^*(f_1 + f_2) \rangle}{\mathcal{N}_{i,j}(f_1, f_2)} \right| \end{aligned} \quad (6)$$

where: \mathcal{N}_{ij} is an appropriate normalization factor (Shahbazi et al., 2014; Chella et al., 2016) that guarantees that ACB is bounded between 0 (i.e., no interaction) and 1 (i.e., maximal interaction); $B_{i,j}(f_1, f_2) = \langle s_i(f_1) s_i(f_2) s_j^*(f_1 + f_2) \rangle$ is the cross-bispectrum between MEG source signals at two locations, location i and location j , respectively; $s_i(f_1)$ and $s_i(f_2)$ are the Fourier coefficients of signal components in source i at frequencies f_1 and f_2 ; $s_j(f_1 + f_2)$ is the Fourier coefficient of signal component in source j at frequency $f_1 + f_2$; $*$ denotes the complex conjugation; $\langle \cdot \rangle$ denotes the expectation value.

A non-vanishing ACB necessarily reflects brain interactions as opposite to the mixing artifacts (Chella et al., 2014) since it cannot be generated by non-interacting sources.

Since we were interested in assessing alpha-beta cross-frequency coupling, we further restricted the components at frequencies f_1 and f_2 to the alpha frequency range (8–12 Hz), and accordingly the component at

frequency $f_1 + f_2$ laid in the beta frequency range (16–24 Hz). Based on this, hereinafter the former two components f_1 and $f_1 + f_2$ will be simply referred to as alpha components and the latter as beta component.

For an efficient computation of the ACB, the cross-bispectral densities and the signal Fourier coefficients were first estimated at the sensor-level and then projected at the source-level through a spatial filter. The cross-bispectral densities and Fourier coefficients used for the ACB calculation in this study were estimated from the data in the pre-cue and in the cue-target interval, for the alpha components (frequencies f_1 and f_2) and for the beta component (frequency f_3) with 1 Hz frequency resolution, after sensor data dimensionality reduction by Principal Component Analysis to the 50 principal components (corresponding to retaining on average about 95% of variance for each subjects). A broadband spatial filter was then constructed by using a time-domain LCMV beamforming (Van Veen et al., 1997). To this end, the covariance matrix for the calculation of the beamformer weights, was estimated within a 0.5 Hz–100 Hz frequency band and from the data in all time windows and all trial conditions. Tikhonov regularization was applied to the covariance matrix with a regularization parameter equal to 5% of the average value of auto-covariance across channels. Cross-bispectral densities and signal Fourier coefficients were thus beamformed onto the vertices of the source space grid, with the source orientation at each vertex being assumed as the one of maximum power (Van Veen et al., 1997).

Cross-frequency connectivity between the two reference regions in frontal areas, located in the proximity of left and right frontal eye fields (lFEF and rFEF), and a given target brain voxel was thus assessed as the average across the ACB values obtained between all the voxels within the FEF region and the target voxel. The motivation for choosing FEFs as seeds for this analysis is that FEFs are well known to be involved in the top-down control of spatial attention (Corbetta and Shulman, 2002). Moreover, while occipital areas have a clear alpha band signature, frontal areas have been associated to both alpha and beta frequencies (Buschman and Miller, 2007; Bastos et al., 2015; Siegel et al., 2008), thus a cross-frequency coupling approach is necessary to assess connectivity to the FEF.

Specifically, the frontal areas were centered at MNI coordinates [-22 6 57] and [22 6 57] respectively and include the voxel at the specified location with the addition of its 6 nearest neighboring voxels, i.e., resulting in a total amount of 7 voxels per region.

Average was also performed across all frequencies f_1 and f_2 in the range 8–12 Hz (i.e., reflecting the coupling with frequencies f_3 in the range 16–24 Hz, thus allowing to investigate an alpha-beta cross-frequency coupling), i.e., $\text{ACB}_{\text{FEF},j}$, for the “Attend Left” trials and for the “Attend Right” trials, separately. The modulation of ACB connectivity induced by the cue presentation was assessed by a contrast between the ACB connectivity in the cue-target interval and the ACB connectivity in the baseline period for each condition, i.e.,

$$\text{mACB}_{\text{FEF},j}^{\text{AttendLeft}} = \text{ACB}_{\text{FEF},j}^{\text{AttendLeft}} - \text{ACB}_{\text{FEF},j}^{\text{Baseline AttendLeft}} \quad (7)$$

and, similarly, for the Attend Right condition.

A conjunction analysis was performed to assess common patterns of alpha-beta connectivity with respect to the FEFs induced by the cue presentation in both conditions. The steps of obtaining the group statistic of the ACB modulation are given in the Experimental Design and Statistical Analysis section. Additionally, in analogy to the definition of the fcAMI for the attentional modulation of the mMIM, we evaluated if the mACB between frontal and parietal areas in the right or in the left hemisphere was modulated by the side to which attention was directed and, possibly, evaluate its hemispheric asymmetry.

2.4. Diffusion MRI

Diffusion MRI analysis procedure closely followed that of Thiebaut de Schotten and colleagues (Thiebaut de Schotten et al., 2011) and was used to dissect the three branches of the SLF: SLF1, SLF2, and SLF3. An index

of hemispheric asymmetry for the three tracts SLF1, SLF2, and SLF3, was computed as:

$$SLF_{asymmetry} = \frac{Volume_{LeftBranch} - Volume_{RightBranch}}{Volume_{LeftBranch} + Volume_{RightBranch}} \cdot 100 \quad (8)$$

where *Volume* refers to the number of voxels intersected by either the Left or the Right branch. Details on acquisition parameters and analysis steps can be found in [Marshall et al. \(2015\)](#).

2.5. Hemispheric asymmetries of alpha band functional connectivity modulation and correlation analyses

To investigate whether attentional modulations of alpha band functional connectivity between occipital regions and regions modulated by the cue presentation (fcAMI_{SOC,X}) are hemispherically lateralized, we computed for each subject a hemispheric asymmetry index according to:

$$\Delta fcAMI_{SOC,X} = fcAMI_{ISOC,IX}^{AttendRight-AttendLeft} - fcAMI_{rSOC,rx}^{AttendLeft-AttendRight} \quad (9)$$

Firstly, we checked whether our population showed a preferential hemispheric lateralization for the attentional modulation of connectivity by running a *t*-test against the hypothesis of no hemispheric lateralization. Then, for the 26 out of 28 subjects having DTI data, we aimed at investigating whether the hemispheric asymmetry of fcAMI was related to the hemispheric asymmetry of the three tracts of the Superior Longitudinal Fasciculus by running a Spearman correlation analysis between SLF_{asymmetry}, separately for each branch, and $\Delta fcAMI_{SOC,PL}$.

Moreover, to assess the degree to which subjects differentially performed in the “Attend Left” versus the “Attend Right” condition, we used the accuracy index (Acc) which, for each condition ($Acc^{AttendLeft}$ and $Acc^{AttendRight}$), is equal to the fraction of correctly reported target orientations. We finally quantified an attentional asymmetry index for the accuracy according to the formula:

$$Acc_{asym} = Acc^{AttendLeft} - Acc^{AttendRight} \quad (10)$$

Finally, in order to understand whether the hemispheric asymmetry for the attentional modulation of functional connectivity is relevant to the subjects' performance, we run a Spearman correlation analysis between $\Delta fcAMI_{SOC,PL}$ and the Acc_{asym} . Along the same line, we tested if the hemispheric asymmetry for the SLF1, SLF2, and SLF3 tracts was correlated with the Acc_{asym} .

2.6. Experimental Design and Statistical Analysis

All the analyses were performed by using MATLAB version R2012b (The MathWorks, Inc., Natick, MA, USA). MEG data preprocessing, sensor-level analysis, and spatial filter estimation were done by using the Fieldtrip software toolbox ([Oostenveld et al., 2011](#)). Source connectivity analysis was performed by using a custom MATLAB code developed by the authors.

The contrast between different experimental conditions across subjects (i.e., MIM or ACB in the cue-target interval versus baseline) relied on paired sampled *t*-test statistics. Statistical significance of the observed differences was assessed by setting a critical threshold (e.g., $p < 0.05$), and the *t*-scores exceeding this threshold were considered as significant. To correct for multiple comparisons, we used the cluster-based permutation approach ([Maris and Oostenveld, 2007](#)) implemented in Fieldtrip. Using this approach, *t*-scores exceeding the critical threshold were clustered based on their spatial adjacency, and the summed *t*-value from the cluster was computed. Then, data from the two experimental conditions were randomly permuted 10,000 times within every subject, and a cluster *t*-value was computed for each randomization, creating a reference distribution of cluster *t*-values under the null hypothesis of no difference between the two experimental conditions. The *p*-value associated with the initial cluster *t*-value was evaluated with respect to this

reference distribution.

The statistical significance of fcAMI_{SOC,X} was assessed by a *t*-test against the null hypothesis of no attentional modulation (i.e., fcAMI = 0). The multiple comparison problem was addressed by using a False Discovery Rate (FDR) approach.

In our analysis, the PSI was used to infer the dominant direction of alpha band connectivity. Statistical significance of PSI was assessed by averaging PSI values and normalizing the result by the standard deviation across subjects. Under the assumption that the normalized values are drawn from a zero-mean normal distribution, the values exceeding a critical threshold value corresponding to a *p*-value of 0.05, averaged over a region of interest, were considered as significant.

To assess common patterns of alpha-beta connectivity with respect to the FEFs induced by the cue presentation in both conditions, a conjunction analysis was performed. The group statistic of the ACB modulation for each FEF region was obtained through the following steps: i) the values of mACB were computed for each voxel and for each condition; ii) a statistically significant threshold for the conjunction of the two conditions, corrected for family-wise error rate, was set by using the method of minimum statistics compared to the global null ([Friston et al., 1999](#)). The voxels at which the mACB exceeded this threshold were assigned a value of 1, while all other voxels were set to 0 to generate binary masks for the “Attend Left” and for the “Attend Right” conditions; iii) a binary valued conjunction mask was obtained by combining the single condition binary masks by a logical AND; iv) the group averaged mACB was computed for each condition and then averaged across the two conditions; and v) the final map was obtained by masking the average obtained in iv) with the conjunction mask derived in iii).

Finally, correlations between functional and structural connectivity, as well as correlations between functional connectivity and behavioral performance, were assessed by using Spearman's rank-order correlation. The *p*-values associated to correlation coefficients were corrected for multiple comparisons by using the FDR approach.

2.7. Data and code availability statement

The data set used in this study have also been used in [Marshall et al. \(2015\)](#) and is therefore already deposited in the Dryad Data Repository: <https://datadryad.org/resource/doi:10.5061/dryad.bt7v0> ([Marshall et al., 2015b](#)). The functional connectivity results and the code used in the study are available upon direct request. Conditions for sharing or re-use include citation of the related papers and comply with CC BY-NC-ND 4.0 licensing and with the requirements of the funding bodies and with institutional ethics approval.

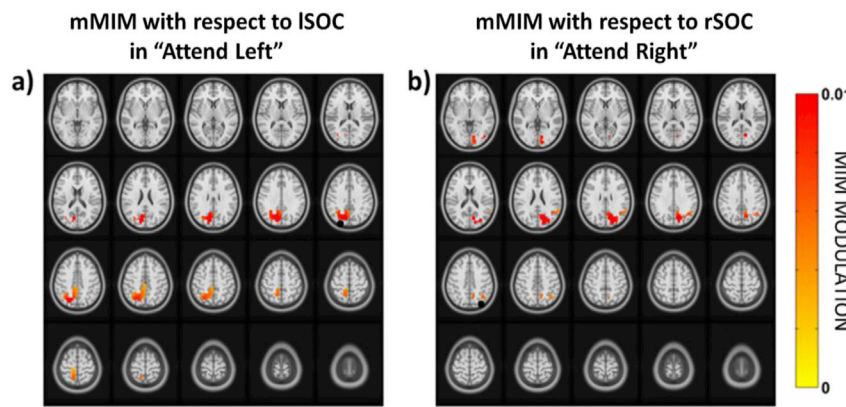
3. Results

Magnetoencephalographic data from 28 subjects performing a cued attention task were analyzed (earlier analysis of same data presented in [Marshall et al., 2015](#)). Analysis of the behavioral data confirmed that spatial cueing improved accuracy and reduced reaction time of target detection compared to neutral conditions ([Marshall et al., 2015](#)).

3.1. Alpha oscillations demonstrate hemisphere-specific parieto-occipital connectivity

Our results in [Fig. 2](#) show a significant increase of connectivity after the cue presentation between the ISOC and a region centered in the left Superior Parietal Lobule (ISPL), as defined according to the AAL parcellation, for the “Attend Left” condition versus Baseline ([Fig. 2a](#)). Similarly, for “Attend Right” versus Baseline we observed a significant increase of connectivity between the rSOC and a region of the right Inferior Parietal Lobule (riPL) ([Fig. 2b](#)).

Interestingly, in both hemispheres, the modulation of MIM between SOC and Parietal Lobule (PL) is still significant after regressing out the alpha power modulation in occipital and parietal cortices (left



hemisphere: $p = 0.0280$; right hemisphere: $p = 0.0307$), suggesting that connectivity was not fully driven by power changes (Figs. S4 and S5 in the Supplementary Material and related text further elaborate on this topic).

The Parietal Lobule is thus considered as the region X in Equations (4), (5) and (9) for the derivation of the Attentional Modulation Index of functional connectivity and of its hemispheric asymmetry in the following.

When considering the directionality of the observed interaction between the SOC and the ipsilateral Parietal Lobule (PL), we found significant negative PSI values consistently in both hemispheres (PSI between left SOC and left PL: 1.84, $p = 0.03$, corrected); PSI between right SOC and right PL: -2.02, $p = 0.02$, corrected). Thus, we can conclude that PLs lead SOCs, possibly accounting for a feedback drive underlying the observed parieto-occipital alpha band interaction.

The same analyses for the MIM and mMIM conducted in the beta band

Fig. 2. Alpha band modulation of the Multivariate Interaction Measure. a) Grand average across subjects of whole brain modulated MIM (mMIM) with respect to the ISOC region (indicated by the black dot) for the "Attend Left" condition versus Baseline; b) Grand average across subjects of whole brain mMIM with respect to the rSOC region (indicated by the black dot) for the "Attend Right" condition versus Baseline. Maps show only statistically significantly modulated voxels (paired t -test, $p < 0.05$ corrected). A significant increase in within-hemisphere parieto-occipital connectivity was found ipsilaterally to the side to which attention had been directed.

did not show significant patterns of functional connectivity modulations.

3.2. Frequency specificity of the parieto-occipital connectivity

The frequency specificity of the observed parieto-occipital connectivity modulations was evidenced by the Time Frequency (TF) analysis of the modulated MIM. Fig. 3a, left panel, shows that the connectivity increase between the occipital cortex and the parietal cortex in the left hemisphere after the cue presentation for the "Attend Left" condition occurs only in the alpha band. When considering the TF analysis of the MIM between the same regions in the "Attend Right" condition, no modulation by the cue presentation is observed nor in alpha neither in any other frequency band (Fig. 3a, right panel). Specularly, the frequency specificity to the alpha band can be observed for the right hemisphere occipito-parietal connectivity modulation in the "Attend Right" (Fig. 3b, right panel), but not in the "Attend Left" condition (Fig. 3b, left panel).

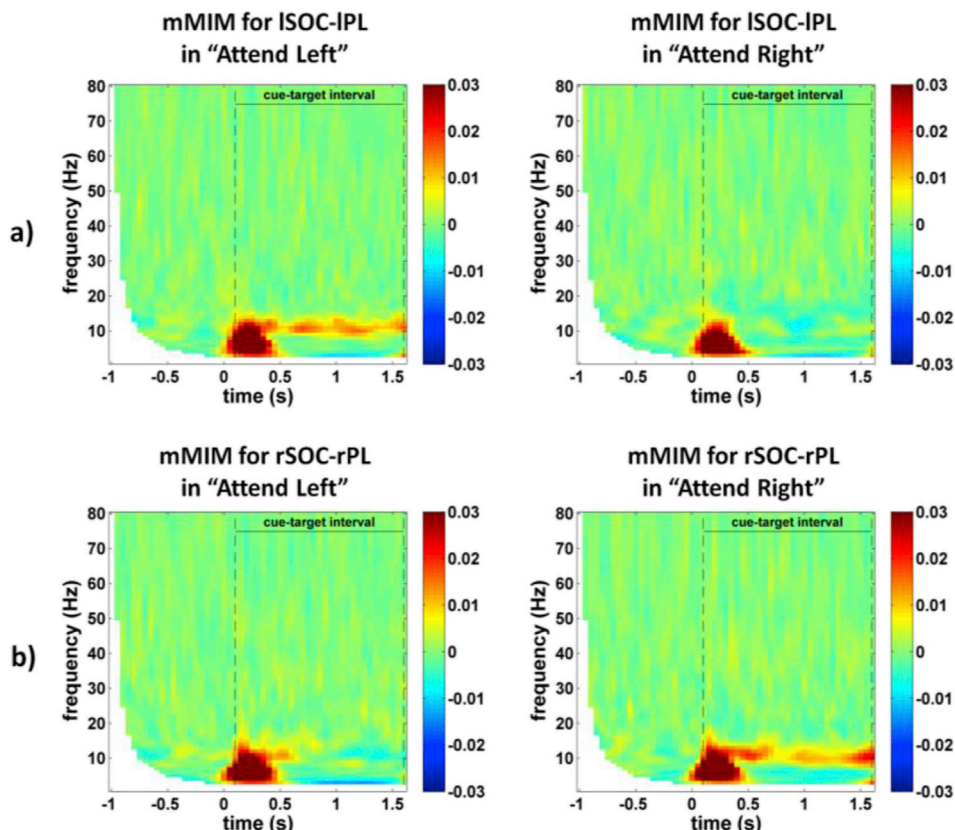


Fig. 3. Time Frequency Representation (TFR) of the occipito-parietal connectivity modulations (mMIM).

In all TFR plots, the time axis is defined such that zero corresponds to the cue presentation and all the other time points are consistent with the time axis of Fig. 1 a) Grand average across subjects of mMIM between the left SOC region and the left PL region in the “Attend Left” condition (left panel) and in the “Attend Right” condition (right panel); b) Grand average across subjects of mMIM between the right SOC region and the right PL region in the “Attend Left” condition (left panel) and in the “Attend Right” condition (right panel). The TFR plots show that increase of mMIM within the cue-target interval is specific for the alpha frequency band and is observed only for connectivities between regions ipsilateral to the attended hemifield, i.e. for ISOC-IPL in “Attend Left” and for rSOC-rPL in “Attend Right”.

Maps show only statistically significantly modulated voxels (paired *t*-test, $p < 0.05$ corrected). A significant increase in within-hemisphere parieto-occipital connectivity was found ipsilateral to the side to which attention had been directed.

3.3. Alpha band parieto-occipital connectivity modulates with direction of attention

The hemisphere-specific cue induced modulation of functional connectivity maps in Fig. 2 suggests a spatial selectivity role for the interplay between parietal cortex and occipital visual regions. The analysis of the Attentional Modulation Index (fcAMI) allowed us to further investigate the spatial selectivity of the interplay between parietal cortex and occipital visual regions. Indeed, the fcAMI indicates a significant negative modulation of connectivity between the SOC and the parietal cortex in both hemispheres. Fig. 4 shows the box plots for the left hemisphere, $\text{fcAMI}_{\text{ISOC,IPL}}^{\text{AttendRight-AttendLeft}}$, and right hemisphere, $\text{fcAMI}_{\text{rSOC,rPL}}^{\text{AttendLeft-AttendRight}}$, respectively. Given that we defined the fcAMI indices always as the occipito-parietal functional connectivity when attending contralaterally to the reference region minus the functional connectivity when attending ipsilaterally to the reference region, the negative sign points out that alpha band functional connectivity between SOC and parietal cortex is always larger when the cue is presented ipsilaterally to the occipital cortex reference region. This supports the hypothesis of a role of parietal areas in functional inhibition of ipsilateral

occipital cortices through phase coherence related to the orienting of attention.

3.4. SLF1 and SLF2 asymmetry predict alpha-band parieto-occipital functional connectivity

The Hemispheric Modulation Asymmetry Index (ΔfcAMI) was used to examine whether the observed ipsilateral attentional modulation of functional connectivity is related to the asymmetry of the SLF tracts. Our findings, illustrated in Fig. 5, show that individual values of Hemispheric Asymmetries for the SLF1 and SLF2 negatively correlate with the hemispheric asymmetry of fcAMI (SLF1: $p = -0.40$, $p = 0.02$, corrected; SLF2: $p = -0.41$, $p = 0.02$, corrected). Given that the values of fcAMI between occipital and parietal cortices were found to be negative, which indicates that in each hemisphere the connectivity is larger when attending to the ipsilateral hemifield, the above negative correlations should be interpreted as a positive relationship between the hemispheric asymmetry of fiber tracts and the hemispheric asymmetry of functional connectivity modulation. For example, a subject whose SLF1 and SLF2 tract volume are larger in the left than in the right hemisphere ($\text{SLF tract asymmetry} > 0$) has also larger connectivity attentional modulation in the left than in the right hemisphere ($\Delta\text{fcAMI} < 0$) and is thus represented by a dot in the upper left quadrant of Fig. 5 panels a) and b).

Of note, the previous analysis of the hemispheric asymmetry of alpha band power modulated by attention in the same data (Marshall et al., 2015) detected a significant correlation with the SLF1 only. Thus, whilst SLF1 asymmetry is linked to both asymmetry in the attentional modulation of alpha power in the occipital cortex and attentional modulation of parieto-occipital alpha band functional connectivity, asymmetry of the SLF2 branch is only related to the latter.

3.5. Asymmetry of functional connectivity predicts attentional biases

We next sought to understand whether individual asymmetries in attentional modulation of parieto-occipital alpha band functional connectivity (ΔfcAMIs) were also related to differences in the accuracy of target discrimination across hemifields. The Spearman rank correlation analysis between ACC_{asym} and hemispheric asymmetry of connectivity modulation between SOC and PL (ΔfcAMI) indicated a significant negative correlation ($p = -0.35$, $p = 0.03$), as reported in Fig. 6. The negative sign of the correlation means that subjects that have a larger functional connectivity modulation in the left than in the right hemisphere (i.e., $\Delta\text{fcAMI} < 0$) respond more accurately to targets presented in the left than in the right hemifield (i.e., $\text{ACC}_{\text{asym}} > 0$). Vice versa, subjects who have a larger functional connectivity modulation in the right hemisphere respond more accurately to targets presented in the right hemifield. For example, a subject who has larger connectivity attentional modulation in the left than in the right hemisphere ($\Delta\text{fcAMI} < 0$) is more accurate when responding to targets presented in the left hemisphere and is thus represented by a dot in the upper left quadrant of Fig. 6.

No significant rank correlation was found between ACC_{asym} and the hemispheric asymmetry of any of the SLF tracts (i.e., ACC_{asym} and $\text{SLF1}_{\text{tract asymmetry}}$: $p = 0.56$; ACC_{asym} and $\text{SLF2}_{\text{tract asymmetry}}$: $p = 0.62$; ACC_{asym} and $\text{SLF3}_{\text{tract asymmetry}}$: $p = 0.70$), indicating that functional connectivity asymmetry, although being related to structural connectivity asymmetry, is more directly associated to task performance than to structural connectivity asymmetry.

3.6. Alpha-beta cross-frequency interactions reveal a right-hemisphere-dominant fronto-parietal network

Finally, we investigated whether the observed parieto-occipital interactions are part of a large-scale circuit also involving frontal areas. Indeed, previous literature highlighted that higher order regions, such as the observed parietal areas but also the frontal eye-fields (FEFs) exert a

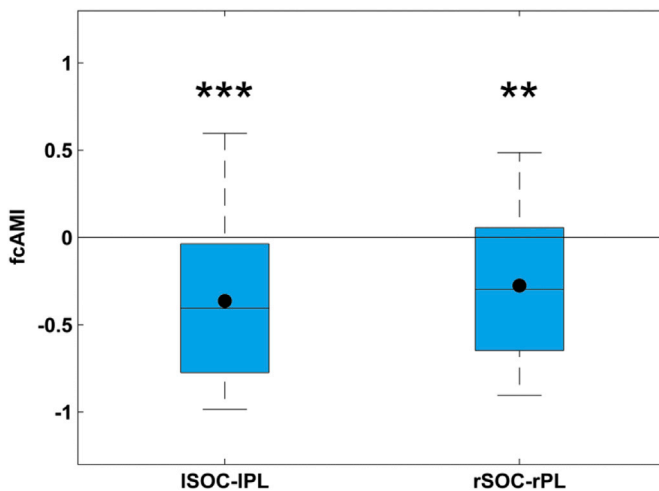


Fig. 4. Box plot of Attentional Modulation Index for connectivity (fcAMI) between SOC and PL for left and right hemispheres, respectively. The middle, bottom, and top of each rectangular box represent the median, 25th percentile, and 75th percentile, respectively, of the distribution of fcAMI across subjects. The black dots represent the mean values. A significant modulation of functional connectivity was found for both hemispheres (** $p = 0.0001$, ** $p = 0.0011$, *t*-test, corrected). The observed negative values reflect an increment of alpha band functional connectivity in the hemisphere ipsilateral to the hemifield indicated by the cue.

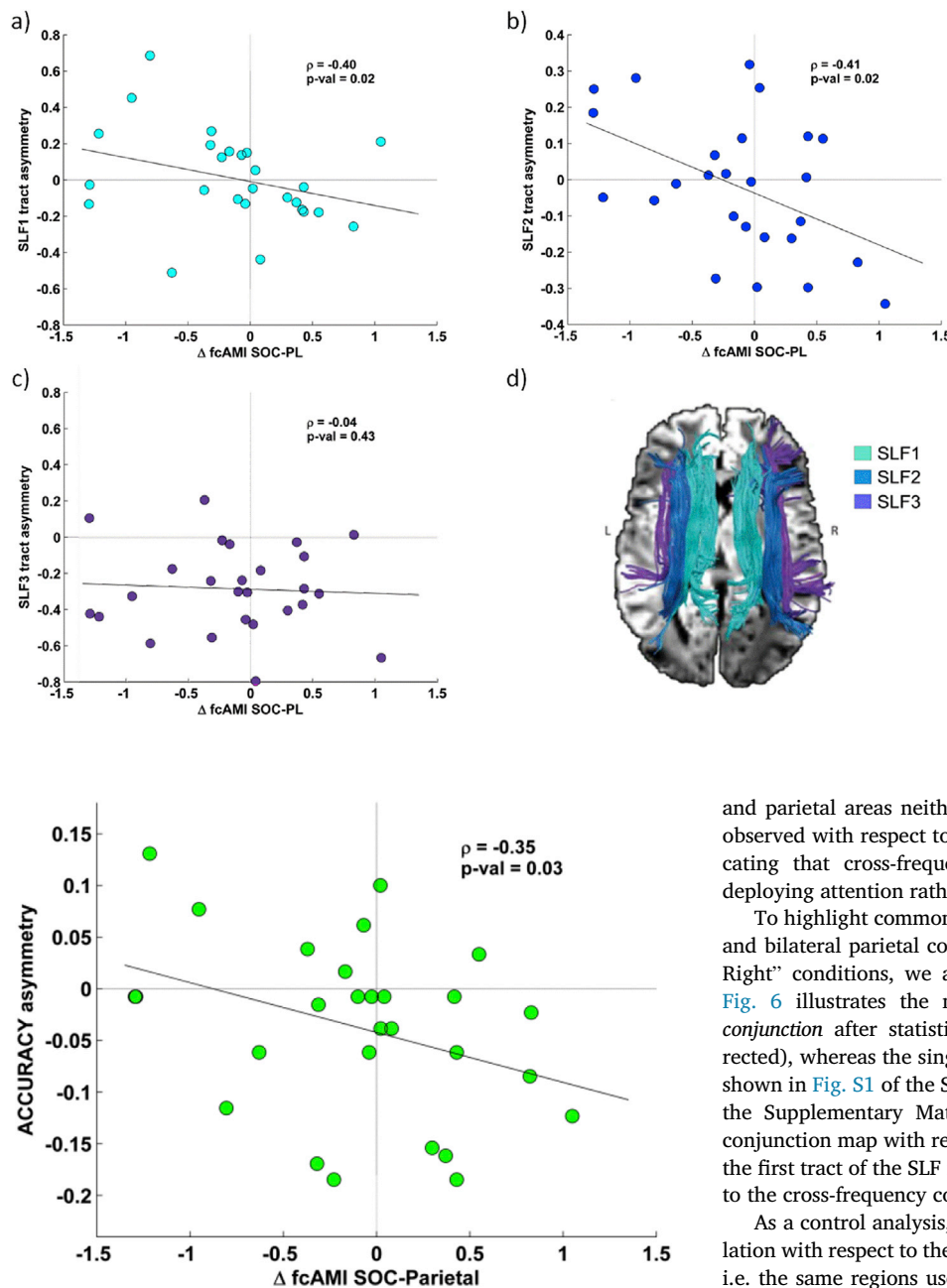


Fig. 5. Relation between SLF tracts hemispheric asymmetries and hemispheric asymmetry of alpha band functional connectivity. a, b, c) Spearman correlation between individual Δ fcAMI and SLF tract asymmetries: a) SLF1 b) SLF2 c) SLF3; Hemispheric Asymmetries of SLF1 and SLF2 tracts correlate with the hemispheric asymmetry of functional connectivity Δ fcAMI ($p = 0.02$, corrected); d) Tractography render of SLF branches in one subject obtained using diffusion MRI. The negative values indicate that subjects have a larger functional connectivity modulation in the hemisphere in which larger tracts volume of SLF1 and SLF2 are present.

Fig. 6. Relation between accuracy asymmetry and hemispheric asymmetry of alpha band functional connectivity. Spearman correlation between individual accuracy asymmetry and the hemispheric asymmetry of fcAMI, i.e., Δ fcAMI ($p = 0.03$). The negative p value indicates that subjects perform better in terms of accuracy when the cue points at the hemifield ipsilateral to the hemisphere that shows the larger connectivity modulation.

top-down control over the modulations in the visual cortex. To this end, the ACB analysis was run by choosing as reference regions bilateral frontal areas, in proximity of the FEFs (Olesen et al., 2003; Marshall et al., 2015). This analysis revealed an increase of the alpha-beta ACB coupling between the right FEF and bilateral parietal areas induced by cue presentation in either hemifield.

No alpha-beta ACB coupling modulation with respect to the left FEF was observed with the same approach, possibly indicating that specific role of the right FEF in the interaction with bilateral parietal cortices in the alpha-beta cross frequency coupling. The results for a control analysis of possible power-induced effects is shown in Fig. S6.

Additionally, no significant modulation of the mACB between frontal

and parietal areas neither in the left nor in the right hemisphere was observed with respect to the side to which attention was directed, indicating that cross-frequency coupling works as mechanism for the deploying attention rather than for orienting attention.

To highlight common patterns of connectivity between the right FEF and bilateral parietal cortices across the “Attend Left” and the “Attend Right” conditions, we applied a conservative conjunction procedure. Fig. 6 illustrates the map of ACB modulation obtained from this conjunction after statistical thresholding ($p < 0.05$, paired t -test, corrected), whereas the single maps used to build the conjunction map are shown in Fig. S1 of the Supplementary Material. Additionally, Fig. S2 of the Supplementary Material shows the overlap between the mACB conjunction map with respect to the right FEF of Fig. 7 and the fibers of the first tract of the SLF in the right hemisphere which connect the rFEF to the cross-frequency coupled parietal regions.

As a control analysis, we calculated alpha-beta ACB coupling modulation with respect to the reference regions located in the bilateral SOCs, i.e. the same regions used to assess alpha band mMIM functional connectivity. In this case, we did not observe any alpha-beta ACB coupling modulation.

To reconcile these findings with the alpha band findings, in Fig. S3 of the Supplementary Material we show the parietal regions (in green) which are concurrently coupled to the occipital cortex in the alpha band and to the right frontal cortex through an alpha-beta cross-frequency mechanism. Additionally, the Supplementary Material Fig. S7 shows the alpha-beta frequency specificity of the observed effects.

4. Discussion

In the present study, we show that functional connectivity, measured as phase synchronization, between occipital and ipsilateral parietal areas in the alpha but not in the beta band is modulated by visuospatial attention, reflecting a control mechanism exerted by parietal regions for the inhibition of visual cortices, as demonstrated by the Phase Slope Index result. Indeed, this occipito-parietal network is specific to the orienting of attention since a larger alpha band connectivity modulation is observed in the hemisphere ipsilateral to the hemifield to which

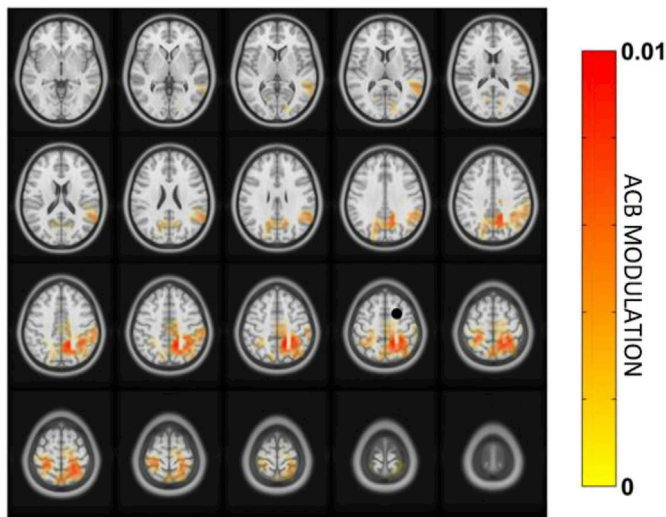


Fig. 7. Conjunction map of ACB modulation versus Baseline for "Attend Left" and "Attend Right" conditions in the alpha-beta band with respect to the right frontal cortex reference region. Maps show only statistically significantly modulated voxels (paired *t*-test, $p < 0.05$ corrected). A significant modulation of the connectivity between right frontal (indicated by the black dot) and bilateral parietal areas was observed.

attention is directed. Importantly, this occipito-parietal functional connectivity modulation is related to the anatomical characteristics of Superior Longitudinal Fasciculus (SLF) tracts, since it exhibits a hemispheric asymmetry which is predicted by the asymmetry in the volume of the first and second SLF tracts, and it is related to performance. Additionally, the alpha-beta bicoherence analysis highlights an involvement of cross-frequency coupling within the fronto-parietal network. In this coupling, the putative right Frontal Eye Field (rFEF) deserves a specific role in the deployment of spatial attention, as indicated by an increased coupling between rFEF and bilateral parietal cortices either when the subject is attending to the left or to the right hemisphere.

Notably, our results highlight, for the first time to our knowledge, a role of individual subject asymmetries in the volume of both the first and the second tract of the SLF in serving asymmetries of alpha band functional connectivity modulation between occipital and parietal cortices. These results are in line with a previous report on the role of SLF asymmetries in visuospatial attention. Indeed, [Marshall et al. \(2015\)](#) demonstrated on the same data used in the present study that the individual differences in SLF1 volume impact on local visual cortical power oscillations acting as a mediation of the top-down control from the prefrontal drive within the dorsal network. Our results on the relation between SLF1 and occipito-parietal functional connectivity complement and extend these findings, demonstrating that a larger number of connections to the frontal cortex could result into increased signal transmission to visual cortex mediated by the parietal cortex, further highlighting the involvement of the dorsal network (and thus SLF1) in this mechanism. Additionally, our result on the relationship between individual differences in SLF2 and occipito-parietal functional connectivity is in line with the study from [Thiebaut de Schotten et al. \(2011\)](#), where the role of SLF2 asymmetry in predicting attentional task performance was shown. Indeed, the authors reported that SLF2 operates as a bridge between the dorsal and ventral networks, acting as a mediator for reorienting goal-directed attention, a process ascribed to SLF1 and the dorsal network, to salient events detected by the ventral attention network.

According to theories of the control of visuospatial attention ([Corbetta and Shulman, 2002](#); [Kastner and Ungerleider, 2000](#)), effective goal-directed behavior is instantiated through the interplay between the visual cortex and a fronto-parietal circuit. However, in our study we observed no alpha fronto-parietal nor fronto-occipital connectivity

modulation, but only a clear modulation of alpha band functional connectivity between parietal cortices and ipsilateral occipital visual area. On the other hand, other human and monkey studies have revealed that the fronto-parietal circuit responding to goal directed attention shows synchronization in the beta frequency range ([Buschman and Miller, 2007](#); [Siegel et al., 2008](#)). Yet, we did not observe any beta band fronto-parietal connectivity modulation. A possible reason why this connectivity was not observed here is that the coupling with respect to the frontal regions does not occur in a linear fashion, rather it requires a non-linear synchronization involving more than one frequency band for each region. This hypothesis is in line with the empirical observations that the frequencies related to top-down influences over the visual cortex differ across the studies between alpha and beta, and the specific role of the alpha and beta bands is not yet clear ([Fries et al., 2015](#)). Our findings support the hypothesis that rather than showing a specific alpha or beta frequency signature, the fronto-parietal circuit is recruited through an alpha-beta cross-frequency synchronization mechanism. In fact, we report a robust alpha-beta cross frequency coupling between frontal and parietal cortices which might represent the broadcast mechanism by which the fronto-parietal circuit operates, whilst the parietal cortex concurrently drives the occipital cortex in the alpha band. Conceivably, the former circuit is related to the deployment of attention, whereas the latter is associated to the process of spatially orienting selective attention. Our findings contribute to reconcile previous results of inter-areal phase synchronization in the alpha to beta range between regions in the attention networks. In this framework, it should be noted that while our results are obtained in a cohort of 28 subjects, while previous observations ([Siegel et al., 2008](#); [Sacchet et al., 2015](#); [Lobier et al., 2018](#)) used fewer subjects, i.e., at most fourteen.

Additionally, our alpha-beta synchronization highlights that the putative right frontal eye field (rFEF) deserves a specific role in the alpha-beta synchronization in comparison to its left hemisphere homologous region. In fact, while the alpha band connectivity modulation of the parieto-occipital circuit was observed in the hemisphere ipsilateral to the attended hemifield, the cross-frequency fronto-parietal circuit involves only the frontal cortex in the right hemisphere. This laterality is in line with the evidence that the right FEF is particularly critical for top-down control of attention to both visual fields ([Esterman et al., 2015](#); [Hung et al., 2011](#); [Silvanto et al., 2006](#)). Along this line, TMS over right frontal cortex has been shown to be more effective than TMS over left frontal cortex in supporting spatial attention process ([Grosbras and Paus, 2003](#); [Capotosto et al., 2009](#)). Moreover, rFEF has recently been found to exert a feedback control on the modulation of alpha band activity in early visual areas ([Popov et al., 2017](#)). Consistently with the latter study, the involvement of the rFEF that we observed is independent of the direction of attention, supporting the hypothesis that this region has a key role in the deployment of spatial attention. A similar role for the right frontal cortex was also found in ([Simpson et al., 2011](#)) using an event-related field approach.

Our alpha-beta synchronization between rFEF and parietal cortex in the right hemisphere is conceivably mediated by the first tract of the SLF in the right hemisphere, as clearly suggested by the overlap between the anterior and posterior terminus of the SLF and the observed functional modulation of ACB (Fig. S3). Conversely, inter-hemispheric association pathways are the possible route through which the parietal cortex in the left hemisphere is recruited. Our hypothesis is that the inter-hemispheric association pathways that support the observed coupling to the left parietal cortex are the callosal pathways rather than extra-callosal routes, consistent with recent findings showing that a section of the corpus callosum markedly reduces inter-hemispheric functional connectivity especially in associative areas in the frontal and parietal lobe ([Roland et al., 2017](#)).

Taken together, the results of our study suggest that alpha oscillations in the parietal cortex act as a bridge in linking the right frontal cortex (characterized by an alpha-beta oscillatory signature) to the visual cortex (characterized by alpha band oscillations), in line with a putative role of

this region as interface between sensory processing and action preparation (Baldauf et al., 2006). The cortical circuit underlying the visuospatial attention process could be obtained in our study only by the concurrent use of linear and nonlinear approaches for estimating functional connectivity. The former highlights the frequency specific alpha band signature of the parieto-occipital subsystem, and the latter highlights the alpha-beta cross-frequency signature of the fronto-parietal subsystem. From a methodological and signal analysis point of view, we wish thus to stress the complementary nature of the information that be gathered by the using both approaches for the characterization of brain networks by magnetoencephalography or electroencephalography, in light with the view of the brain instantiating concurrent coupling modes at different temporal scale/frequencies (Engel et al., 2013). It is thus likely that our findings about network subsystems indexed by characteristic spectral fingerprints with different functional roles, different relation to anatomy, and different behavioral relevance, can be generalized to other cognitive process. In this framework, it is likely that higher order areas might coordinate the involvement of the different network subsystems through cross-frequency coupling mechanisms (Nikulin and Brismar, 2006).

Finally, it should be noted that, whilst our study demonstrates that spatial attention processes are effectively mediated by a circuit of cortico-cortical connections, it is important to consider that also cortico-subcortical structures, such as the pulvinar or the nucleus accumbens, play a role in visuospatial attention, i.e., by routing the synchronization between different cortical regions (Saalmann et al., 2012; Horschig et al., 2015; Zhou et al., 2016). In this regard, we must note that the use of MEG allows to only reliably measure the activity of neocortical sources. Indeed, the sensitivity of MEG rapidly decreases as the sources are located deeper inside the brain, thus limiting our capability to observe subcortical structures. Therefore, despite the clear advantage offered by MEG in exploring neuronal oscillations at the same temporal scale of behavior (i.e., in the millisecond time range), it must be noted that our findings by no means can exclude a role for subcortical regions.

Acknowledgements

This work was partially funded by the 2017 Faculty Research Grant of the University of Chieti-Pescara from author LM entitled "Methods for the study of functional connectivity in Magnetoencephalography and Electroencephalography and applications to neuroscience" and by the Netherlands Organization for Scientific Research NWO Grant (453-09-002). Author ADA is supported by Bial Foundation Grant for Scientific Research, grant number 66/16 by author LM. Author FC is supported by BREAKBEN-H2020-FETOPEN-2014-2015/H2020-FETOPEN-2014-2015-RIA, the content of this paper reflects only the authors' view and the European Commission is not responsible for it. In addition, we would like to thank Carlo Sestieri for his comments on an early version of this manuscript and Alessio Basti for his comments on data analysis.

Appendix A. Supplementary data

Supplementary data to this article can be found online at <https://doi.org/10.1016/j.neuroimage.2018.12.056>.

References

- Andreou, C., Leicht, G., Nolte, G., Polomac, N., Moritz, S., Karow, A., Hangani-Opatz, I.L., Engel, A.K., Mulert, C., 2015. Resting-state theta-band connectivity and verbal memory in schizophrenia and in the high-risk state. *Schizophr. Res.* 161 (2–3), 299–307. <https://doi.org/10.1016/j.schres.2014.12.018>.
- Baldauf, D., Wolf, M., Deubel, H., 2006. Deployment of visual attention before sequences of goal-directed hand movements. *Vis. Res.* 46, 4355–4374. <https://doi.org/10.1016/j.visres.2006.08.021>.
- Basti, A., Pizzella, V., Chella, F., Romani, G.L., Nolte, G., Marzetti, L., 2018. Disclosing large-scale directed functional connections in MEG with the multivariate phase slope index. *Neuroimage* 175, 161–175. <https://doi.org/10.1016/j.neuroimage.2018.03.004>.
- Bastos, A.M., Vezoli, J., Bosman, C.A., Schoffelen, J.M., Oostenveld, R., Dowdall, J.R., De Weerd, P., Kennedy, H., Fries, P., 2015. Visual areas exert feedforward and feedback influences through distinct frequency channels. *Neuron* 85, 390–401. <https://doi.org/10.1016/j.neuron.2014.12.018>.
- Bell, A.J., Sejnowski, T.J., 1995. An information-maximization approach to blind separation and blind deconvolution. *Neural Comput.* 7, 1129–1159. <https://doi.org/10.1162/neco.1995.7.6.1129>.
- Brunetti, M., Marzetti, L., Sepede, G., Zappasodi, F., Pizzella, V., Sarchione, F., Vellante, F., Martinotti, G., Di Giannantonio, M., 2017. Resilience and cross-network connectivity: A neural model for post-trauma survival. *Prog. Neuropsychopharmacol. Biol. Psych.* 77, 110–119. <https://doi.org/10.1016/j.pnpbp.2017.04.010>.
- Buschman, T.J., Miller, E.K., 2007. Top-down versus bottom-up control of attention in the prefrontal and posterior parietal cortices. *Science* 315, 1860–1862. <https://doi.org/10.1126/science.1138071>.
- Bushnell, M.C., Goldberg, M.E., Robinson, D.L., 1981. Behavioral enhancement of visual responses in monkey cerebral cortex. I. Modulation in posterior parietal cortex related to selective visual attention. *J. Neurophysiol.* 46 (4), 755–772. PMID: 7288463.
- Capotosto, P., Babiloni, C., Romani, G.L., Corbetta, M., 2009. Frontoparietal cortex controls spatial attention through modulation of anticipatory alpha rhythms, vol. 29, pp. 5863–5872. <https://doi.org/10.1523/JNEUROSCI.0539-09.2009> (18).
- Chella, F., Marzetti, L., Pizzella, V., Zappasodi, F., Nolte, G., 2014. Third order spectral analysis robust to mixing artifacts for mapping cross-frequency interactions in EEG/MEG. *Neuroimage* 91, 146–161. <https://doi.org/10.1016/j.neuroimage.2013.12.064>.
- Chella, F., Pizzella, V., Zappasodi, F., Nolte, G., Marzetti, L., 2016. Bispectral pairwise interacting source analysis for identifying systems of cross-frequency interacting brain sources from electroencephalographic or magnetoencephalographic signals. *Phys. Rev. E* 93 (5), 052420. <https://doi.org/10.1103/PhysRevE.93.052420>.
- Colclough, G.L., Brookes, M.J., Smith, S.M., Woolrich, M.W., 2015. A symmetric multivariate leakage correction for MEG connectomes. *Neuroimage* 117, 439–448. <https://doi.org/10.1016/j.neuroimage.2015.03.071>.
- Corbetta, M., Shulman, G.L., 2002. Control of goal-directed and stimulus-driven attention in the brain. *Nat. Rev. Neurosci.* 3, 201–215. <https://doi.org/10.1038/nrn755>.
- Doesburg, S.M., Green, J.J., McDonald, J.J., Ward, L.M., 2009. From local inhibition to long-range integration: functional dissociation of alpha-band synchronization across cortical scales in visuospatial attention. *Brain Res.* 1303, 97–110.
- Engel, A.K., Fries, P., Singer, W., 2001. Dynamic predictions: oscillations and synchrony in top-down processing. *Nat. Rev. Neurosci.* 2, 704–716.
- Engel, A.K., Gerloff, C., Hilgetag, C.C., Nolte, G., 2013. Intrinsic coupling modes: multiscale interactions in ongoing brain activity. *Neuron* 80, 867–886. <https://doi.org/10.1016/j.neuron.2013.09.038>.
- Esterman, M., Liu, G., Okabe, H., Reagan, A., Thai, M., DeGutis, J., 2015. Frontal eye field involvement in sustaining visual attention: Evidence from transcranial magnetic stimulation. *Neuroimage* 111, 542–548. <https://doi.org/10.1016/j.neuroimage.2015.01.044>.
- Ewald, A., Marzetti, L., Zappasodi, F., Meinecke, F.C., Nolte, G., 2012. Estimating true brain connectivity from EEG/MEG data invariant to linear and static transformations in sensor space. *Neuroimage* 60, 476–488. <https://doi.org/10.1016/j.neuroimage.2011.11.084>.
- Fonov, V.S., Evans, A.C., McKinstry, R.C., Almlie, C.R., Collins, D.L., 2009. Unbiased nonlinear average age-appropriate brain templates from birth to adulthood. *Neuroimage* 47 (Suppl. 1). S102ISSN 1053-8119. [https://doi.org/10.1016/S1053-8119\(09\)70845-5](https://doi.org/10.1016/S1053-8119(09)70845-5).
- Fonov, V.S., Evans, A.C., Botteron, K., Almlie, C.R., McKinstry, R.C., Collins, D.L., 2011. Unbiased average age-appropriate atlases for pediatric studies. *Neuroimage* 54, 313–327. <https://doi.org/10.1016/j.neuroimage.2010.07.033>.
- Fries, P., 2005. A mechanism for cognitive dynamics: neuronal communication through neuronal coherence. *Trends Cognit. Sci.* 9, 474–480. <https://doi.org/10.1016/j.tics.2005.08.011>.
- Fries, P., 2015. Rhythms for Cognition: Communication through Coherence. *Neuron* 7 (1), 220–235. <https://doi.org/10.1016/j.neuron.2015.09.034>, 88.
- Friston, K., Holmes, A., Price, C., Buechel, C., Worsley, K., 1999. Multisubject fMRI studies and conjunction analyses. *Neuroimage* 10, 385–396. <https://doi.org/10.1006/nimg.1999.0484>.
- Gross, J., Kujala, J., Hamalainen, M., Timmermann, L., Schnitzler, A., Salmelin, R., 2001. Dynamic imaging of coherent sources: studying neural interactions in the human brain. *Proc. Natl. Acad. Sci. Unit. States Am.* 98 (2), 694–699. <https://doi.org/10.1073/pnas.98.2.694>.
- Gross, J., Baillet, S., Barnes, G.R., Henson, R.N., Hillebrand, A., Jensen, O., Jerbi, K., Litvak, V., Maess, B., Oostenveld, R., Parkkonen, L., Taylor, J.R., van Wassenhove, V., Wibral, M., Schoffelen, J.-M., 2013. Good practice for conducting and reporting MEG research. *Neuroimage* 65, 349–363. <https://doi.org/10.1016/j.neuroimage.2012.10.001>.
- Grosbras, M.H., Paus, T., 2003. Transcranial magnetic stimulation of the human frontal eye field facilitates visual awareness. *Eur. J. Neurosci.* 18 (11), 3121–3126. <https://doi.org/10.1111/j.1460-9568.2003.03055.x>.
- Horschig, J.M., Smolders, R., Bonnefond, M., Schoffelen, J.-M., van den Munckhof, P., Schuurman, P.R., Cools, R., Denys, D., Jensen, O., 2015. Directed Communication between Nucleus Accumbens and Neocortex in Humans Is Differentially Supported by Synchronization in the Theta and Alpha Band. *PLoS One* 10 (9). <https://doi.org/10.1371/journal.pone.0138685>, e0138685.
- Hung, J., Driver, J., Walsh, V., 2011. Visual selection and the human frontal eye fields: effects of frontal transcranial magnetic stimulation on partial report analyzed by Bundesen's theory of visual attention. *J. Neurosci.* 31, 15904–15913. <https://doi.org/10.1523/JNEUROSCI.2626-11.2011>.

- Jensen, O., Mazaheri, A., 2010. Shaping functional architecture by oscillatory alpha activity: gating by inhibition. *Front. Hum. Neurosci.* 4, 186. <https://doi.org/10.3389/fnhum.2010.00186>.
- Jensen, O., Bonnefond, M., Marshall, T.R., Tiesinga, P., 2015. Oscillatory mechanisms of feedforward and feedback visual processing. *Trends Neurosci.* 38 (4), 192–194. <https://doi.org/10.1016/j.tins.2015.02.006>.
- Kastner, S., Ungerleider, L.G., 2000. Mechanisms of visual attention in the human cortex. *Annu. Rev. Neurosci.* 23, 315–341. <https://doi.org/10.1146/annurev.neuro.23.1.315>.
- Lobier, M., Palva, J.M., Palva, S., 2018. High-alpha band synchronization across frontal, parietal and visual cortex mediates behavioral and neuronal effects of visuospatial attention. *Neuroimage* 165, 222–237. <https://doi.org/10.1016/j.neuroimage.2017.10.044>.
- Makeig, S., Bell, A.J., Jung, T.-P., Sejnowski, T.J., 1996. Independent component analysis of electroencephalographic data. In: Touretzky, D., Mozer, M., Hasselmo, M. (Eds.), *Advances in Neural Information Processing Systems*, vol. 8. MIT Press, Cambridge, MA, pp. 145–151.
- Maris, E., Oostenveld, R., 2007. Nonparametric statistical testing of EEG- and MEG-data. *J. Neurosci. Methods* 164 (1), 177–190. <https://doi.org/10.1016/j.jneumeth.2007.03.024>.
- Marshall, T.R., Bergmann, T.O., Jensen, O., 2015. Frontoparietal Structural Connectivity Mediates the Top-Down Control of Neuronal Synchronization Associated with Selective Attention. *PLoS Biol.* 13 (10), e1002272. <https://doi.org/10.1371/journal.pbio.1002272>.
- Marshall, T.R., Bergmann, T.O., Jensen, O., 2015b. Data from: Frontoparietal structural connectivity mediates the top-down control of neuronal synchronization associated with selective attention. In: Dryad Digital Repository. <https://doi.org/10.5061/dryad.bt7v0>.
- Marzetti, L., Della Penna, S., Snyder, A.Z., Pizzella, V., Nolte, G., de Pasquale, F., Romani, G.L., Corbetta, M., 2013. Frequency specific interactions of MEG resting state activity within and across brain networks as revealed by the multivariate interaction measure. *Neuroimage* 79, 172–183. <https://doi.org/10.1016/j.neuroimage.2013.04.062>.
- Nikias, C.L., Petroppu, A.P., 1993. *Higher-Order Spectra Analysis: A Nonlinear Signal Processing Framework*. Prentice Hall signal processing series. PTR Prentice Hall, Englewood Cliffs, NJ.
- Nikulin, V.V., Brismar, T., 2006. Phase synchronization between alpha and beta oscillations in the human electroencephalogram. *Neuroscience* 137 (2), 647–657. <https://doi.org/10.1016/j.neuroscience.2005.10.031>.
- Nolte, G., 2003. The magnetic lead field theorem in the quasi-static approximation and its use for magnetoencephalography forward calculation in realistic volume conductors. *Phys. Med. Biol.* 48 (22), 3637–3652. <https://doi.org/10.1088/0031-9155/48/22/002>.
- Nolte, G., Bai, O., Wheaton, L., Mari, Z., Vorbach, S., Hallett, M., 2004. Identifying true brain interaction from EEG data using the imaginary part of coherency. *Clin. Neurophysiol.* 115 (10), 2292–2307. <https://doi.org/10.1016/j.clinph.2004.04.029>.
- Nolte, G., Ziehe, A., Nikulin, V.V., Schlogl, A., Krämer, N., Brismar, T., Müller, K.R., 2008. Robustly estimating the flow direction of information in complex physical systems. *Phys. Rev. Lett.* 100 (23), 234101. <https://doi.org/10.1103/PhysRevLett.100.234101>.
- Olesen, P.J., Nagy, Z., Westerberg, H., Klingberg, T., 2003. Combined analysis of DTI and fMRI data reveals a joint maturation of white and grey matter in a fronto-parietal network. *Cognit. Brain Res.* 18, 48–57. <https://doi.org/10.1016/j.cogbrainres.2003.09.003>.
- Oostenveld, R., Fries, P., Maris, E., Schoffelen, J.-M., 2011. FieldTrip: Open source software for advanced analysis of MEG, EEG, and invasive electrophysiological data. *Comput. Intell. Neurosci.* 156869. <https://doi.org/10.1155/2011/156869>, 2011.
- Palva, S., Palva, J.M., 2012. Discovering oscillatory interaction networks with M/EEG: challenges and breakthroughs. *Trends Cognit. Sci.* 16 (4), 219–230. <https://doi.org/10.1016/j.tics.2012.02.004>.
- Peiker, I., David, N., Schneider, T.R., Nolte, G., Schöttle, D., Engel, A.K., 2015. Perceptual Integration Deficits in Autism Spectrum Disorders Are Associated with Reduced Interhemispheric Gamma-Band Coherence. *J. Neurosci.* 36 (50), 16352–16361. <https://doi.org/10.1523/JNEUROSCI.1442-15.2015>, 35.
- Percival, D.B., Walden, A.T., 1993. *Spectral Analysis for Physical Applications: Multitaper and Conventional Univariate Techniques*. Cambridge University Press, Cambridge.
- Popov, T., Kastner, S., Jensen, O., 2017. FEF-controlled Alpha Delay Activity Precedes Stimulus-induced Gamma Band Activity in Visual Cortex. *J. Neurosci.* 37, 4117–4127. <https://doi.org/10.1523/JNEUROSCI.3015-16.2017>.
- Roland, J.L., Snyder, A.Z., Hacker, C.D., Mitra, A., Shimony, J.S., Limbrick, D.D., Raichle, M.E., Smyth, M.D., Leuthardt, E.C., 2017. On the role of the corpus callosum in interhemispheric functional connectivity in humans. *Proc. Natl. Acad. Sci. U. S. A.* 114 (50), 13278–13283. <https://doi.org/10.1073/pnas.1707050114>.
- Saalmann, Y.B., Pinsk, M.A., Wang, L., Li, X., Kastner, S., 2012. Pulvinar regulates information transmission between cortical areas based on attention demands. *Science* 337 (6095), 753–756. <https://doi.org/10.1126/science.1223082>.
- Sacchet, M.D., LaPlante, R.A., Wan, Q., Pritchett, D.L., Lee, A.K.C., Hämäläinen, M., Moore, C.I., Kerr, C.E., Jones, S.R., 2015. Attention drives synchronization of alpha and beta rhythms between right inferior frontal and primary sensory neocortex. *J. Neurosci.* 35, 2074–2082.
- Salinas, E., Sejnowski, T.J., 2001. Correlated neuronal activity and the flow of neural information. *Nat. Rev. Neurosci.* 2, 539–550.
- Sauseng, P., Klimesch, W., Stadler, W., Schabus, M., Doppelmayr, S., Gruber, W.R., 2005. A shift of visual spatial attention is selectively associated with human EEG alpha activity. *Eur. J. Neurosci.* 22, 2917–2926.
- Schoeffelen, J.M., Gross, J., 2009. Source connectivity analysis with MEG and EEG. *Hum. Brain Mapp.* 30 (6), 1857–1865. <https://doi.org/10.1002/hbm.20745>.
- Shahbazi, F., Ewald, A., Nolte, G., 2014. Univariate normalization of bispectrum using Hölder's inequality. *J. Neurosci. Methods* 233, 177–186. <https://doi.org/10.1016/j.jneumeth.2014.05.030>.
- Siegel, M., Donner, T.H., Oostenveld, R., Fries, P., Engel, A.K., 2008. Neuronal synchronization along the dorsal visual pathway reflects the focus of spatial attention. *Neuron* 60 (4), 709–719. <https://doi.org/10.1016/j.neuron.2008.09.010>.
- Silvanto, J., Lavie, N., Walsh, 2006. Stimulation of the human frontal eye fields modulates sensitivity of extrastriate visual cortex. *J. Neurophysiol.* 96, 941–945. <https://doi.org/10.1152/jn.00015.2006>.
- Simpson, G.V., Weber, D.L., Dale, C.L., Pantazis, D., Bressler, S.L., Leahy, R.M., Luks, T.L., 2011. Dynamic Activation of Frontal, Parietal, and Sensory Regions Underlying Anticipatory Visual Spatial Attention. *J. Neurosci.* 31 (39), 13880–13889. <https://doi.org/10.1523/JNEUROSCI.1519-10.2011>.
- Soto, J.L.P., Lachaux, J.-P., Baillet, S., Jerbi, K., 2016. A multivariate method for estimating cross-frequency neuronal interactions and correcting linear mixing in MEG data, using canonical correlations. *J. Neurosci. Methods* 271, 169–181. <https://doi.org/10.1016/j.jneumeth.2016.07.017>.
- Stolk, A., Todorovic, A., Schoffelen, J.M., Oostenveld, R., 2013. Online and offline tools for head movement compensation in MEG. *Neuroimage* 68, 39–48. <https://doi.org/10.1016/j.neuroimage.2012.11.047>.
- Thiebaut de Schotten, M., Dell'Acqua, F., Forkel, S.J., Simmons, A., Vergani, F., Murphy, D.G.M., et al., 2011. A lateralized brain network for visuospatial attention. *Nat. Neurosci.* 14 (10), 1245–1246. <https://doi.org/10.1038/nrn.2905>.
- Thut, G., Nietzel, A., Brandt, S.A., Pascual-Leone, A., 2006. Alpha-band electroencephalographic activity over occipital cortex indexes visuospatial attention bias and predicts visual target detection. *J. Neurosci.* 26 (37), 9494–9502. <https://doi.org/10.1523/JNEUROSCI.0875-06.2006>.
- Tzourio-Mazoyer, N., Landeau, B., Papathanassiou, D., Crivello, F., Etard, O., Delcroix, N., et al., 2002. Automated anatomical labeling of activations in SPM using a macroscopic anatomical parcellation of the MNI MRI single-subject brain. *Neuroimage* 15 (1), 273–289. <https://doi.org/10.1006/nimg.2001.0978>.
- Van Veen, B.D., Van Dromgelen, W., Yuchtman, M., Suzuki, A., 1997. Localization of brain electrical activity via linearly constrained minimum variance spatial filtering. *IEEE (Inst. Electr. Electron. Eng.) Trans. Biomed. Eng.* 44 (9), 867–880. <https://doi.org/10.1109/10.623056>.
- Varela, F., Lachaux, J., Rodriguez, E., Martinerie, J., 2001. The brain web: phase synchronization and large-scale integration. *Nat. Rev. Neurosci.* 2, 229–239. <https://doi.org/10.1038/35067550>.
- Wyart, V., Tallon-Baudry, C., 2008. Neural dissociation between visual awareness and spatial attention. *J. Neurosci.* 28 (10), 2667–2679. <https://doi.org/10.1523/JNEUROSCI.4748-07.2008>.
- Worden, M.S., Foxe, J.J., Wang, N., Simpson, G.V., 2000. Anticipatory biasing of visuospatial attention indexed by retinotopically specific alpha-band electroencephalography increases over occipital cortex. *J. Neurosci.* 20 (6), RC63. <http://www.jneurosci.org/content/20/6/RC63>.
- Zhou, H., Schafer, J.R., Desimone, R., 2016. Pulvinar-Cortex Interactions in Vision and Attention. *Neuron* 89 (1), 209–220. <https://doi.org/10.1016/j.neuron.2015.11.034>.